JOURNAL OF APPLIED ELECTROCHEMISTRY 23 (1993) 753–759

Electrochemical formation of Ni–Y intermetallic compound layer in molten chloride

G. XIE, K. EMA, Y. ITO

Department of Nuclear Engineering, Faculty of Engineering, Kyoto University, Sakyo-ku, Kyoto 606, Japan

ZHAO MIN SHOU

Changchun Institute of Applied Chemistry, Academia Sinica, Changchun 130022, China

Received 25 February 1992; revised 28 April 1992; accepted 15 May 1992

The reduction of Y(III) ions in molten chloride is known to be a one-step three electron reaction [1, 2, 3], but a voltammogram of YCl_3 in molten LiCl–KCl–NaCl at a nickel electrode shows at least two reduction peaks of Y(III) ions, indicating the possibility of formation of Ni–Y intermetallic compounds. Using a galvanostatic electrolysis method, samples were prepared at several current densities at 450, 500, 600 and 700° C, respectively, and were identified with X-ray diffraction (XRD) and electron probe microanalysis (EPMA) methods. The results show that Ni_2Y, Ni_2Y_3 and NiY can be produced by electrolysis and Ni_2Y is found to be the predominant Ni–Y intermetallic compound under the experimental conditions. Nickel appears to diffuse in Ni_2Y faster than yttrium, and the diffusion process is the rate determining step during Ni_2Y formation.

1. Introduction

Rare earth metals are well known as effective catalysts, and they are also excellent alloying elements. For example, Cr–Ni–Y, Fe–Cr–Al–Y and nickel-base superalloy have been developed as anticorrosive, heat resistant, long service life alloy materials. Considering the good mechanical properties of intermetallic compounds and effective catalytic characteristic of rare earth metals, as well as the existence of many kinds of intermetallic compounds of nickel and yttrium [4], it is not difficult to imagine the possibility of Ni–Y intermetallic compounds as surface functional materials. In this study, an attempt is made to produce Ni–Y intermetallic compound films on nickel surfaces by an electrochemical process in molten chloride.

2. Experimental details

For the experiments carried out at 450–600° C, 55LiCl–36KCl–9NaCl (mol %) eutectic mixture was used as a solvent electrolyte. 50KCl–50NaCl mixture was used for experiments at 700° C. LiCl, KCl and NaCl were all of reagent grade (Wako Chemical Co., Ltd). The anhydrous YCl_3 was obtained by slowly heating a mixture of $YCl_3 \cdot 6H_2O$ and NH_4Cl under vacuum. A molybdenum wire 1 mm in diameter and a nickel disc of 7 mm in diameter were used as the working electrodes. To measure the electrode potential, a stabilized zirconia–air electrode was used as a quasi-reference electrode for convenience [5], and the measured values are presented in the figures relative to the M^+/M electrode potential. Here, M represents an alkali metal (Li and Na), and the potential of M^+/M remains constant, (-3.627 ± 0.006) V(Cl_2/Cl^-), at 450° C, which is the decomposition potential of the solvent [3], though the exact composition of M is not defined. A glassy carbon rod of 5 mm in diameter was used as the counter electrode. The salt mixture was contained in a high purity alumina crucible (99.5% Al_2O_3, Nippon Kagaku Togyo Co., Ltd SSA-S) and was melted under dry argon atmosphere. After anhydrous YCl_3 was added to the eutectic, dry HCl gas was passed through the eutectic for 2 h. Finally, the cell was kept under a slight positive pressure of dry argon gas to keep out atmospheric moisture.

3. Results and discussion

3.1. *Voltammetry*

A typical cyclic voltammogram of Y(III) ion at a nickel electrode obtained at 450° C in the solvent electrolyte with addition of 1.2 mol % YCl_3 is shown in Fig. 1. There are at least two clear reduction peaks at about 300 mV and 400 mV, respectively. Near 0 mV, cathodic breakdown of the electrolyte occurs. However, previous work [3] revealed that the electrochemical reduction of Y(III) in molten 55LiCl–36KCl–9NaCl (mol %) system is a one-step three electron reaction. According to the Ni–Y phase diagram [4], several intermetallic compounds can be formed between nickel and yttrium. The two reduction peaks may be associated with the formation of yttrium and a Ni–Y intermetallic compound, respectively. For comparison, the cyclic voltammogram of the Y(III) ion at a molybdenum electrode, obtained under the same conditions, is also plotted as dashed line in Fig. 1.

0021-891X

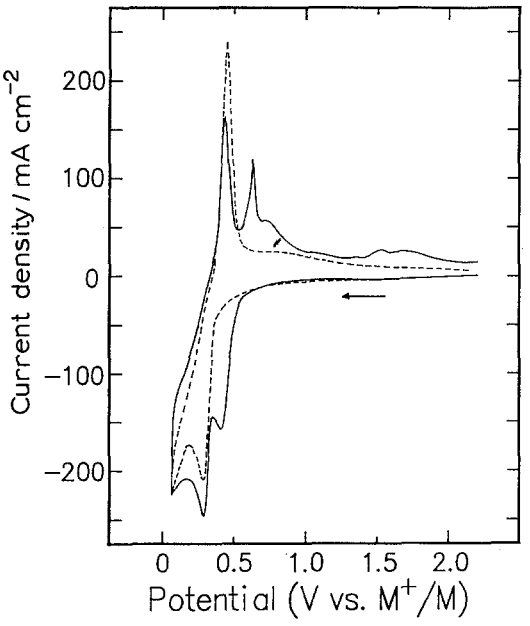

Fig. 1. Voltammograms of Ni (——) and Mo (----) electrodes. (1.2 mol % YCl_3; scanning rate: 100 mV s^{-1}, 450° C).

Because no alloys or intermetallic compounds can be formed between molybdenum and yttrium, only the reduction peak of Y(III) appears. Considering the result for the molybdenum electrode, it seems that the reduction peak at 300 mV, which is just the deposition potential of yttrium at the molybdenum electrode, corresponds to the electrodeposition of yttrium metal, and the other peak corresponds to the direct formation of an Ni–Y intermetallic compound. On the reversal sweep, in addition to the two sharp oxidation peaks, which correspond to the two reduction peaks, there are two other oxidation peaks (shoulders) at about 0.7 V and 1.5 V, though there are no corresponding reduction peaks. These indicate the possibility of formation of more than one kind of Ni–Y intermetallic compounds. The cyclic voltammograms of Y(III) ion at the nickel electrode at 500, 600 and 700° C are all very similar to that obtained at 450° C.

3.2. *Open-circuit potentiometry*

Open-circuit potentiometry was also carried out to confirm the results for the cyclic voltammetry. After galvanostatic electrolysis for 30 s at an electrolysis current density of 800 mA cm^{-2}, the current was interrupted, and the open-circuit potential decay curve of the nickel electrode was measured. The result is shown in Fig. 2. Plateau (a) represents the cathodic breakdown of the electrolyte, and the two plateaus, (b) and (c), correspond to the two sharp oxidation peaks in Fig. 1. Plateau (d), which corresponds to the peak at about 1.5 V, is still not understood. No plateau corresponding to the oxidation peak at about 0.7 V in Fig. 1 appears.

3.3. *Potentiostatic electrolysis*

In order to confirm the inference concerning the two reduction peaks in Fig. 1, potentiostatic electrolysis was conducted near the two peak potentials, i.e. 400 and 310 mV, respectively, at 450° C, with 700 C charge. It should be noted that the charging times are different in these two experiments, since the current densities are different. After electrolysis, the samples were taken out from the bath, and the surfaces of the samples were investigated. A black mud-like deposit was found on the surfaces. The amount of this deposit on the sample prepared at 310 mV was much more than that on the sample prepared at 400 mV. The samples were washed with distilled water and then cleaned in alcohol using an ultrasonic cleaner. Weight increases of these two samples were also measured, as 12 and 0 mg, respectively. The XRD patterns of the two samples are shown in Figs 3 and 4. From the results, it can be seen that the surface of the sample prepared at 400 mV is composed of Ni_2Y and Ni_2Y_3. The cross-section of the sample prepared at 400 mV was analysed quantitatively by EPMA with atomic

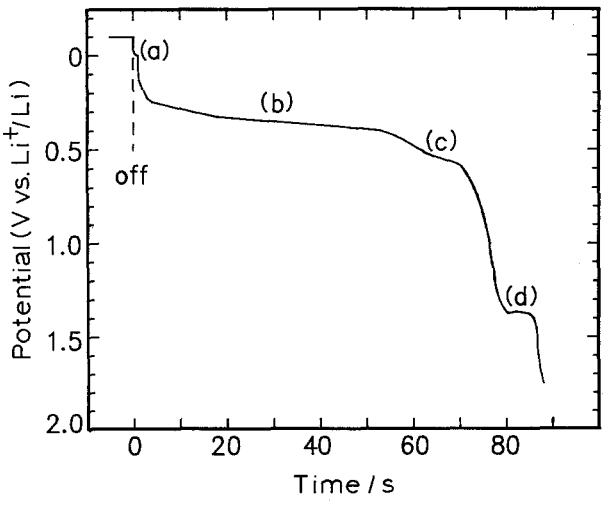

Fig. 2. Open-circuit potential decay curve of Ni electrode after electrolysis at 800 mA cm^{-2} for 30 s. (1.2 mol % YCl_3, 450° C).

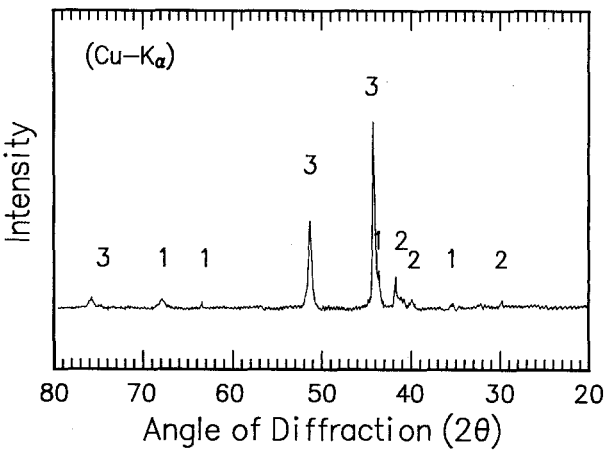

Fig. 3. XRD spectrum of sample prepared at 400 mV for 40 h. (1.2 mol % YCl_3, 700 C charge, 450° C). (1) Ni_2Y, (2) Ni_2Y_3 and (3) Holder (Monel).

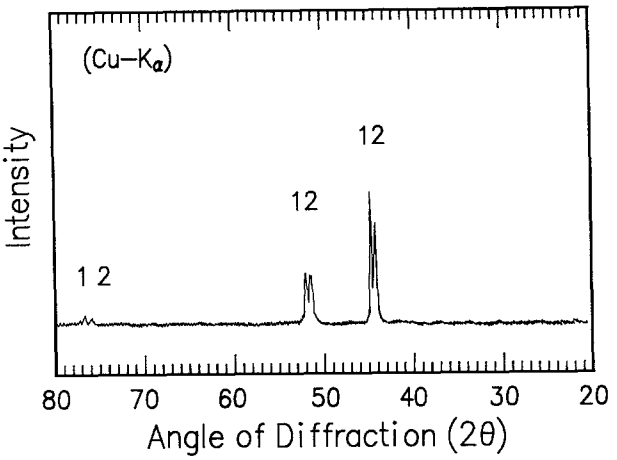

Fig. 4. XRD spectrum of sample prepared at 310 mV for 2.5 h. (1.2 mol % YCl_3, 700 C charge, 450° C). (1) Ni and (2) Holder (Monel).

number(Z)–adsorption–fluorescence(ZAF) correction. The result shows that the bulk product is Ni_2Y. In contrast, nothing was left on the surface of the sample prepared at 310 mV. Judging from the above results, the black mud-like deposit is likely to be yttrium metal. Because of the reactive properties of yttrium metal, the deposited yttrium metal on the samples will react with water and oxygen in the air, when taken out from the bath, and washed out by distilled water after electrolysis. That is why nothing is detected on the surface of the sample prepared at 310 mV. Of course, deposited yttrium can form Ni–Y intermetallic compounds by thermal diffusion, but the total period of the experiment in this case was too short for its formation.

3.4. *Thermal diffusion effect*

To discuss the effect of thermal diffusion, a sample was prepared by potentiostatic electrolysis at 310 mV. In this experiment, however, after passing 1420 C charge, instead of being taken out of the bath immediately, the sample was kept in the bath until the total period was as long as the experiment period for preparation of the sample prepared at 400 mV, and then washed and cleaned in the same way as above. The surface and the cross-section of the sample were then investigated by XRD and EPMA, respectively. The XRD pattern of the sample is shown in Fig. 5: the result reveals that the surface product is NiY. EPMA measurement indicates that the bulk product is Ni_2Y. But the weight increase of the electrode was only 4 mg, which was much smaller than that of the electrode prepared at 400 mV, i.e. 12 mg, though the quantity of charge passed at the former was twice that of the latter. The different weight increases result from the different formation mechanisms.

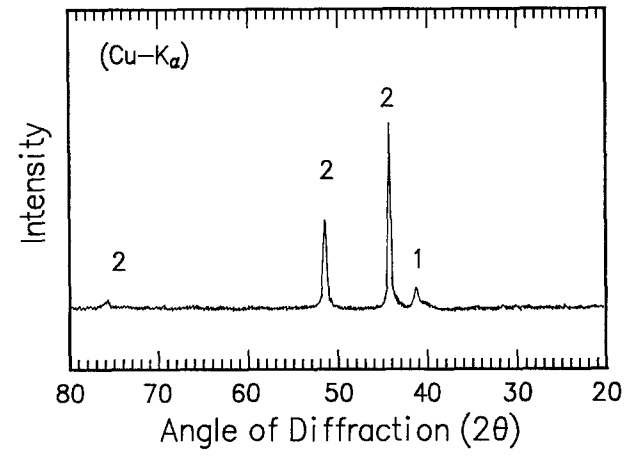

Fig. 5. XRD spectrum of sample prepared at 310 mV and kept in the bath until total experimental period being 40 h. (1.2 mol % YCl_3, 1420 C charge, 450° C). (1) NiY and (2) Holder (Monel).

3.5. *The influence of electrolysis current density and bath temperature*

In order to investigate the effects of electrolysis current densities and bath temperatures, samples were prepared by galvanostatic electrolysis at various current densities at 450, 500, 600 and 700° C. The samples were washed and cleaned in the same way as above. The surfaces were analyzed with XRD, and the cross-sections with ZAF correction EPMA. The results are summarized in Table 1. It can be seen that at 450° C, NiY and Ni_2Y_3 are formed at the surface and the fraction of NiY decreases with increase in current density. On the other hand, Ni_2Y was found as bulk product with no dependence on the current density. At 500, 600 and 700° C, both surface and bulk products are Ni_2Y, being independent of current density, except in the case of 500° C at 200 mA cm^{-2}. It seems that both bath temperature and current density can affect the product composition to some extent, but only in the surface region. Ni_2Y is found to be the predominant Ni–Y intermetallic compound under the experimental conditions.

SEM images of cross-sections of the sample were also taken. Figures 6–9 show the SEM images of cross-sections of the samples prepared at 600° C at electrolysis current densities of 50, 100, 150 and 200 mA cm^{-2}, respectively. In this current density range, the electrode potential stays between the deposition potential of yttrium and the direct formation potential of Ni–Y intermetallic compound, and moves closely to the deposition potential of yttrium with

Table 1. The effects of electrolytic current density and bath temperature

Current density /mA cm⁻²	*Analysis method*	*Bath temperature*			
		450° C	*500° C*	*600° C*	*700° C*
50	XRD	NiY, Ni_2Y_3	Ni_2Y	Ni_2Y	Ni_2Y
	EPMA	Ni_2Y	Ni_2Y	Ni_2Y	Ni_2Y
100	XRD	NiY, Ni_2Y_3	Ni_2Y	Ni_2Y	Ni_2Y
	EPMA	Ni_2Y	Ni_2Y	Ni_2Y	Ni_2Y
150	XRD	NiY, Ni_2Y_3	Ni_2Y	Ni_2Y	Ni_2Y
	EPMA	Ni_2Y	Ni_2Y	Ni_2Y	Ni_2Y
200	XRD	Ni_2Y_3	Ni_2Y, Ni_2Y_3	Ni_2Y	Ni_2Y
	EPMA	Ni_2Y	Ni_2Y	Ni_2Y	Ni_2Y

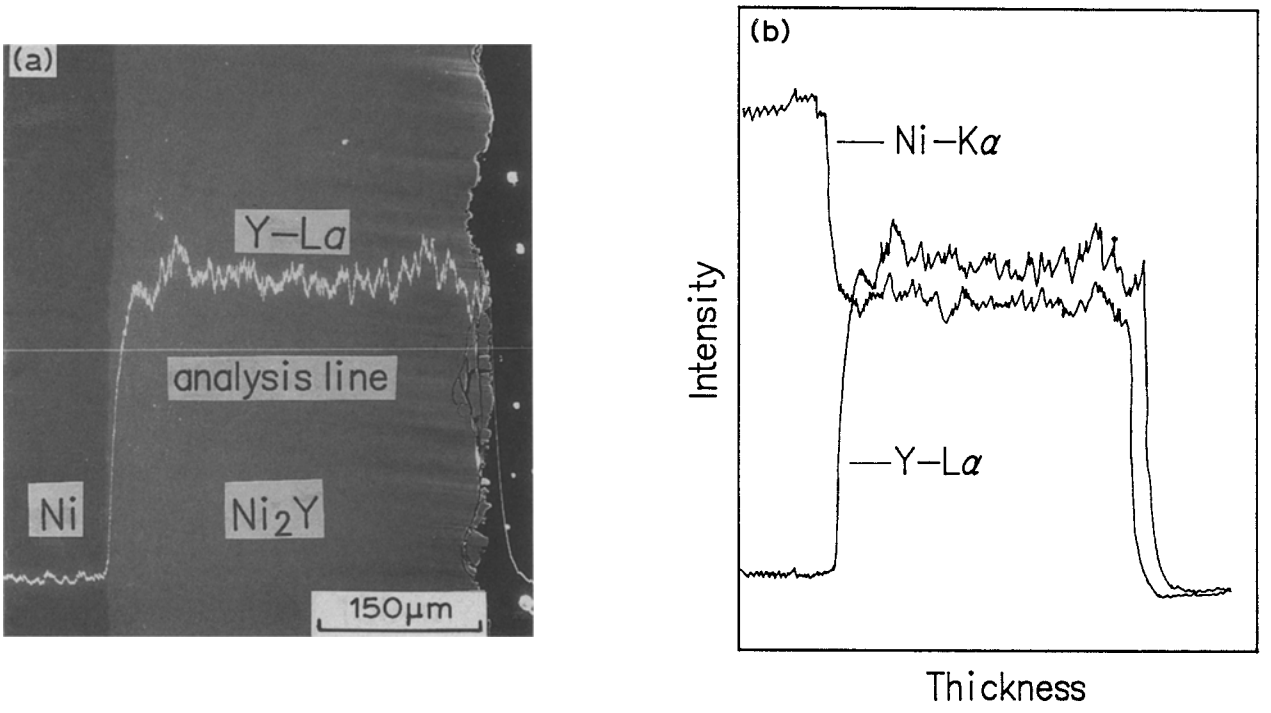

Fig. 6. (a) SEM image of the cross-section of sample prepared at 50 mA cm^{-2}. (b) Concentration profiles of Y and Ni of the cross-section. (1.2 mol % YCl_3, 600° C).

increase of current density. It can be seen from the photos that in all these cases, adhesive uniform Ni_2Y layers were formed. Line analysis of the cross-sections were implemented to identify the existence of Ni_2Y layers. The concentration profiles of Y and Ni are also shown in Figs 6–9. The results of line analysis also prove that the Ni_2Y layers formed are uniform. An adhesive uniform Ni_2Y layer can also be obtained at 500, 600 and 700° C. But the situation at 450° C is different; the deposit layer has a double-layer structure (Fig. 10). The inner layer is only composed of Ni_2Y, but the surface layer seems to be a mixture of

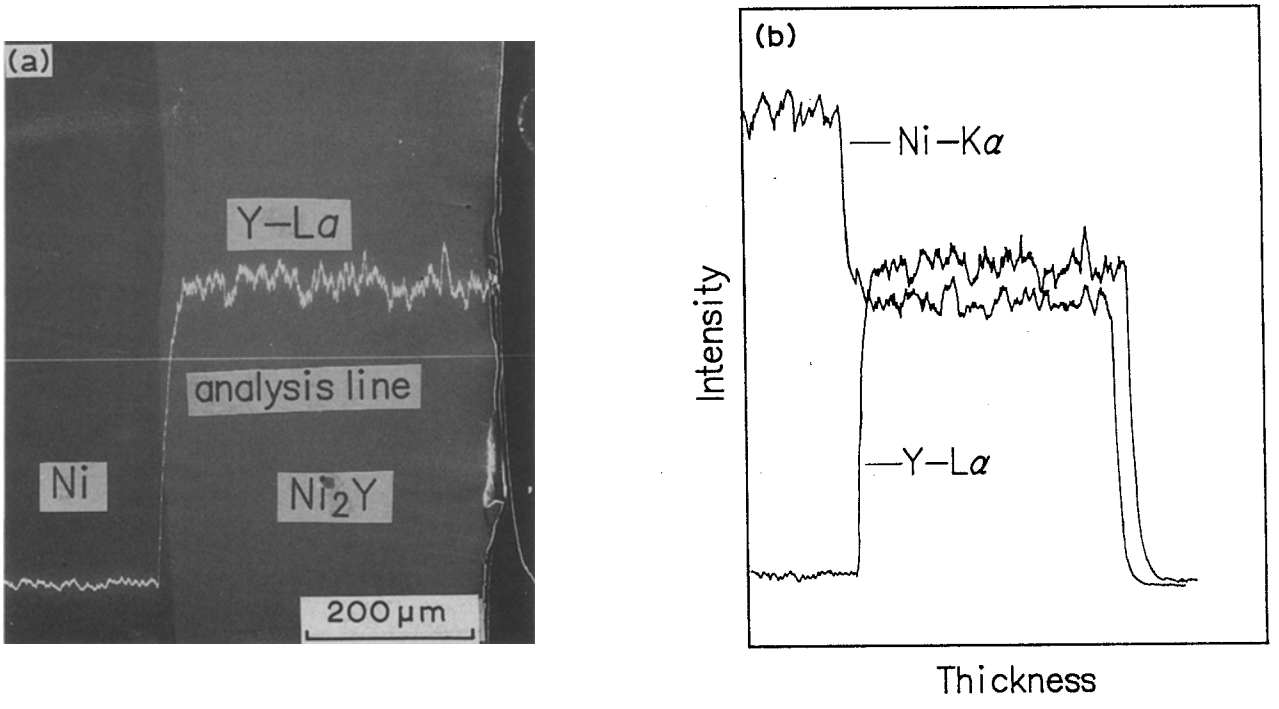

Fig. 7. (a) SEM image of the cross-section of sample prepared at 100 mA cm^{-2}. (b) Concentration profiles of Y and Ni of the cross-section. (1.2 mol % YCl_3, 600° C).

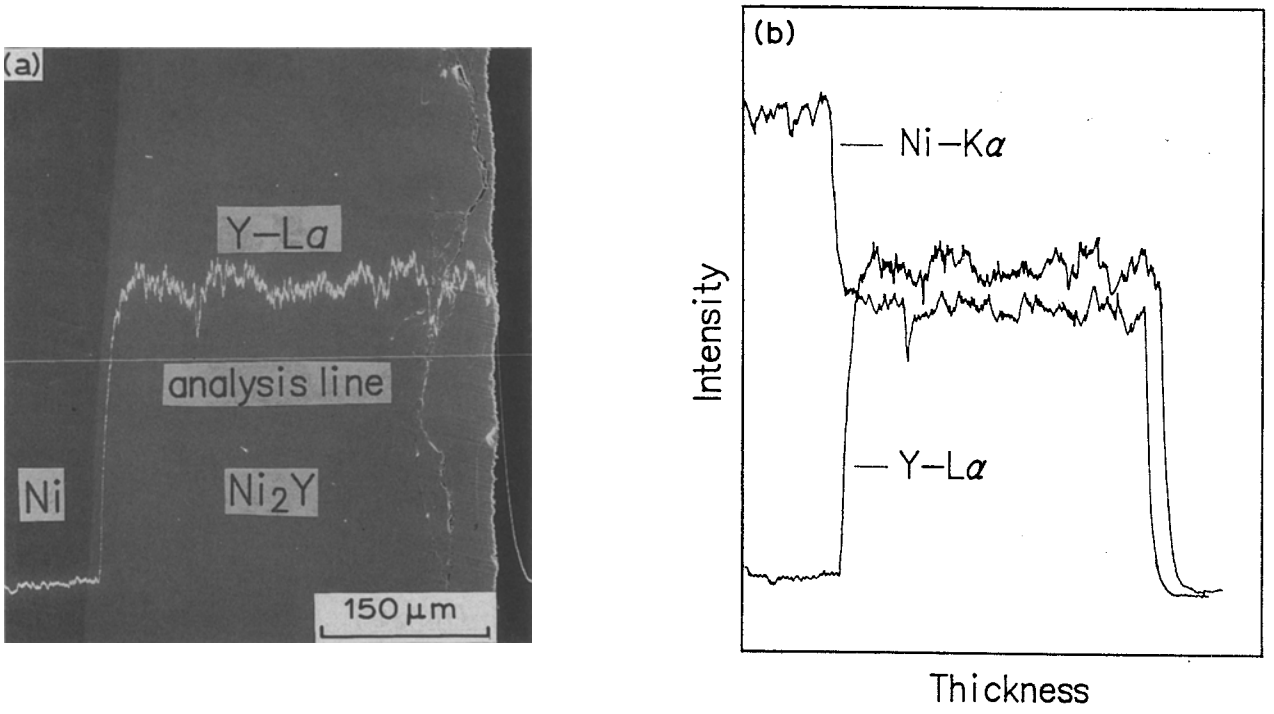

Fig. 8. (a) SEM image of the cross-section of sample prepared at 150 mA cm^{-2}. (b) Concentration profiles of Y and Ni of the cross-section. (1.2 mol % YCl_3, 600° C).

NiY and Ni_2Y_3 and inside this layer there are numerous cracks, which may be caused by the different stresses from the different intermetallic compounds.

Electrolytic current efficiencies were also investigated. When taken out from the bath after electrolysis, the samples were washed and then weighed. The apparent current efficiency was calculated as the ratio of electrode weight increase during the electrolysis to the theoretical weight increase corresponding to all the charge passed through the electrode. Clearly, the real current efficiency will be much larger, since the deposition of yttrium does not contribute to the

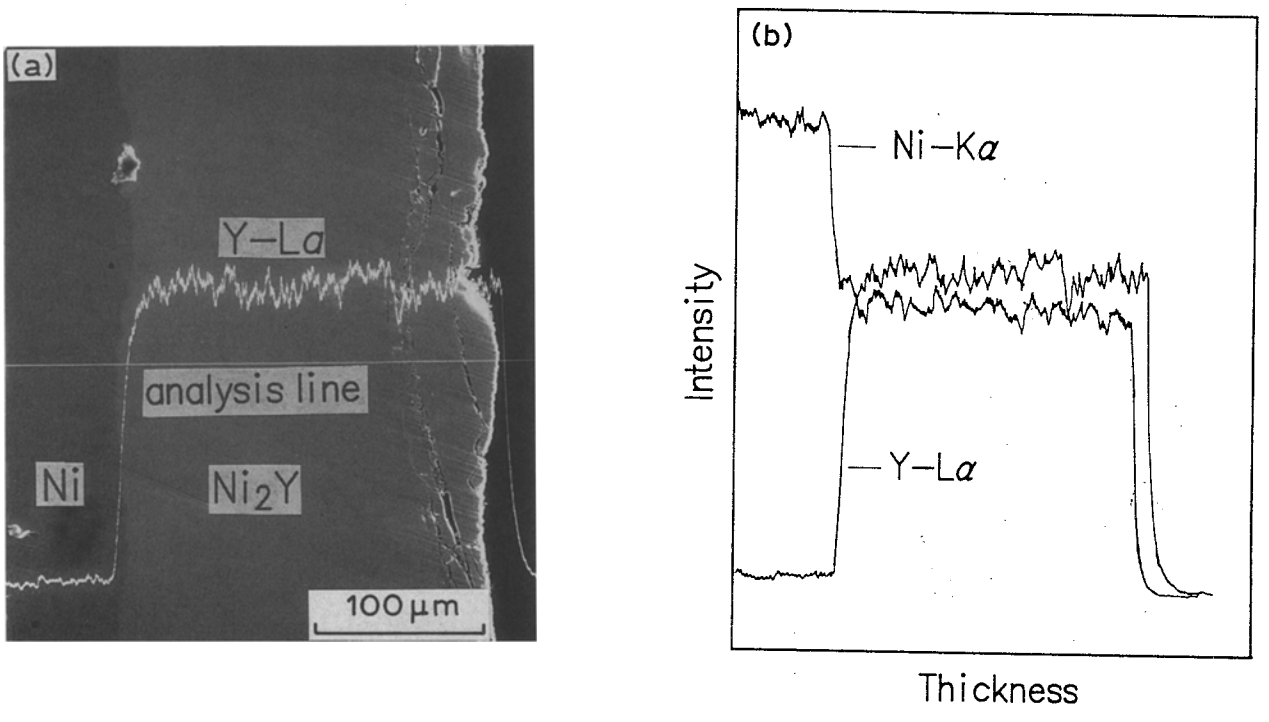

Fig. 9. (a) SEM image of the cross-section of sample prepared at 200 mA cm^{-2}. (b) Concentration profiles of Y and Ni of the cross-section. (1.2 mol % YCl_3, 600° C).

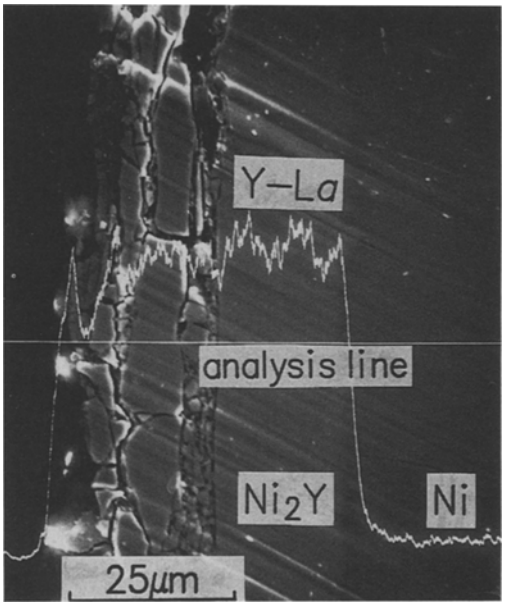

Fig. 10. SEM image of the cross-section of sample prepared at 200 mA cm^{-2}. (1.2 mol % YCl_3, 450° C).

apparent current efficiency. If there is no electrochemical side reaction here, that is, all the charge passed through the electrode is used for the direct formation of Ni–Y intermetallic compounds and the deposition of yttrium, the real current efficiency will be 100%. The results of experiments conducted at 500° C are shown in Fig. 11. It can be deduced that interdiffusion of yttrium and nickel atoms is the rate determining step in the formation of Ni_2Y. When the yttrium deposition rate is larger than the diffusion rate, the larger the electrolysis current density, the greater the accumulation of yttrium on the electrode surface. The accumulated yttrium on the electrode surface reacts with water and oxygen in the air and is washed out by distilled water after electrolysis. So the apparent current efficiency decreases with increase in current density. The influence of bath temperature on electrolysis current efficiency is shown in Fig. 12. The current efficiency increases with increase in bath temperature, since interdiffusion of yttrium and nickel is accelerated as the temperature is raised.

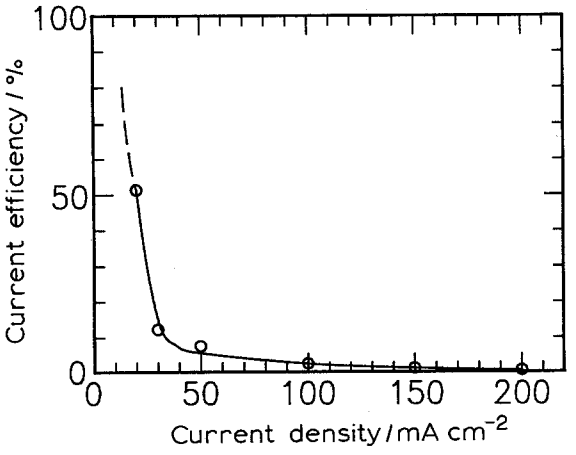

Fig. 11. Electrolytic current efficiency. (1.2 mol % YCl_3, 500° C).

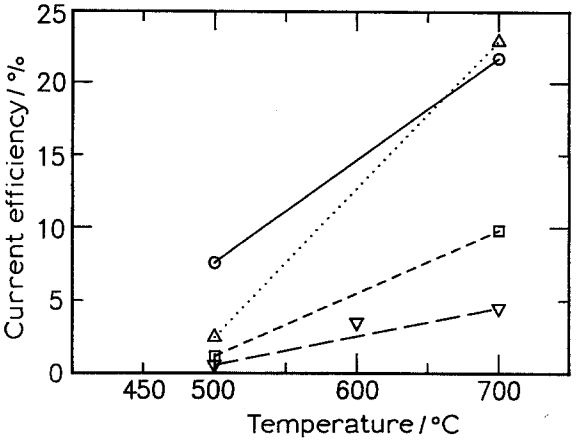

Fig. 12. The influence of bath temperature on electrolytic current efficiency. (1.2 mol % YCl_3). Current density/mA cm^{-2}: (○) 50, (△) 100, (□) 150 and (▽) 200.

3.6. *Interdiffusion of yttrium and nickel*

In order to investigate the interdiffusion of yttrium and nickel during Ni_2Y formation, the following experiment was designed: a tungsten marker, a half-circle shaped film of 0.1 mm in thickness, was fixed on a nickel disc surface by spot welding. Through this film diffusion of both yttrium and nickel could be completely prevented. A sketch of such an electrode before electrolysis is shown in Fig. 13. Using this electrode, galvanostatic electrolysis was carried out for 20 h at a current density of 50 mA cm^{-2} at 500° C. An SEM image of the cross-section of the sample after electrolysis is shown in Fig. 14. Part A in the figure indicates the original position of the tungsten marker. Since the interface between nickel and Ni_2Y is quite hard to see on the micrograph, both being shades of grey, a simple sketch is used to make the point better (Fig. 15). Clearly, the Ni_2Y–Ni interface has moved in the direction of the nickel base. The thickness of the Ni_2Y layer is about 290 μm, and the distance between the Ni_2Y–Ni interface and the original nickel surface is about 210 μm. On the other hand, the left edge of the Ni_2Y layer moved outside by 80 μm from the original nickel surface. Ni_2Y has a fcc crystal structure, which is the same crystal structure as Ni. It appears that nickel diffuses in Ni_2Y faster than yttrium. A quantitative consideration of the intermetallic diffusion phenomenon will constitute a future research subject.

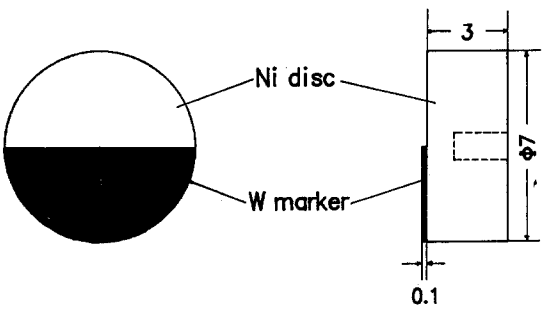

Fig. 13. A sketch of a nickel electrode with a tungsten marker.

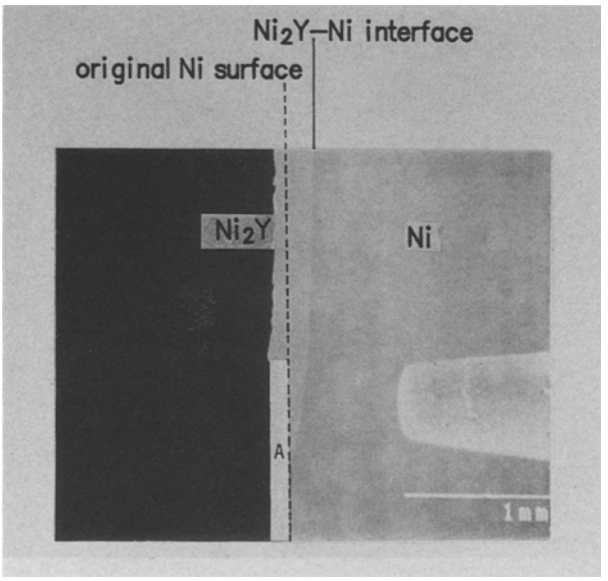

Fig. 14. SEM image of the cross-section of the sample with a tungsten marker after electrolysis. (1.2 mol% YCl_3, 500° C, 50 mA cm^{-2}, 24 h).

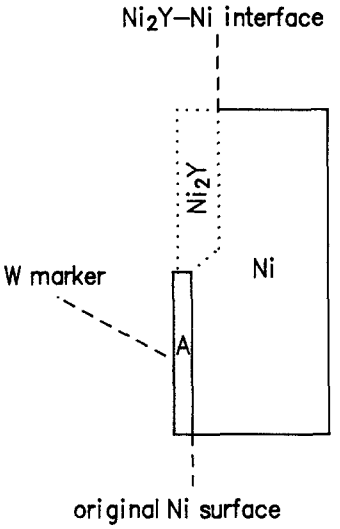

Fig. 15. A sketch of the micrograph of Fig. 14.

4. Conclusion

The voltammogram of YCl_3 in molten LiCl–KCl–NaCl at a nickel electrode showed the possibility of formation of Ni–Y intermetallic compounds. Using galvanostatic electrolysis, samples were prepared at several electrolytic current densities at 450, 500, 600 and 700° C, respectively, and were identified with XRD and EPMA. The results show that Ni_2Y, Ni_2Y_3 and NiY can be produced by electrolysis and Ni_2Y, which is formed in bulk independent of bath temperature and current density, is found to be the predominant Ni–Y intermetallic compound. Bath temperature and current density affect the composition of the product to some extent, but only in the surface region under the present experimental conditions. Rather thick adhesive uniform Ni_2Y layers can be obtained in the bath temperature range 500–700° C at all the experimental current densities investigated. Nickel appears to diffuse in Ni_2Y faster than yttrium, and the diffusion process is the rate determining step in Ni_2Y formation.

Acknowledgement

The work was supported by a grant-in-aid from the Japanese Ministry of Education, Science and Culture. The authors thank Mr Teruyoshi Unezaki of Kyoto University for the measurements of SEM and EPMA. The authors also thank Mr Koji Yoshida of Kyoto University for his help and support of this work.

References

[1] L. Yang and R. G. Hudson, *Trans. Metall. Soc. AIME* **215** (1959) 589.
[2] Y. Hoshino and J. A. Palmbeck, *Can. J. Chem.* **48** (1970) 685.
[3] Z. M. Shou, S. Hikino, G. Xie, K. Ema and Y. Ito, *J. Electrochem. Soc.*, in preparation.
[4] O. Izumi, 'Intermetallic Compound' (in Japanese), Sangyo-Toshyo Inc. (1988).
[5] J. Shiokawa, *Denki Kagaku* **58** (1990) 702.
[6] T. B. Massalski, J. L. Murray, L. H. Bennett and H. Baker, 'Binary Alloy Phase Diagrams', American Society for Metals (1987) p 1775.
[7] Y. Ito, H. Yabe, T. Nakai, K. Ema and J. Oishi, *Electrochimica Acta* **31** (1986) 1579.